GENERAL RESEARCH

Stability of the Steady Motion of a Liquid Plug in a Capillary Tube

Diego M. Campana,[†,‡] Sebastián Ubal,[†,‡] María D. Giavedoni,*[,‡] and Fernando A. Saita[‡]

Facultad de Ingeniería, Universidad Nacional de Entre Ríos, Ruta Prov. 11, km 10, 3101 Oro Verde, Entre Ríos, Argentina and INTEC, CONICET, Universidad Nacional del Litoral, Güemes 3450, 3000 Santa Fe, Argentina

In this work, we present a methodology to analyze the stability of the steady-state propagation of a liquid plug in a capillary tube lined with a uniform film of the same liquid. To this end, the steady-state solutions are computed and the corresponding film thickness is obtained for different plug lengths and fixed capillary and Reynolds values. The evolution of this variable as a function of the plug length for each capillary and Reynolds number is the key to plug stability determination.

1. Introduction

The motion of a liquid plug inside a capillary tube is a problem associated with both biological phenomena and technological applications. An example of the former is the liquid plug formed either when a liquid is instilled into the respiratory airways for therapeutic purposes or during the expiration process as a consequence of a capillary instability of the liquid film lining the wall of the smallest airway conduits. Microchannel reactors illustrate the latter.

A simplified model of these problems is the propagation of a volume of liquid inside a capillary tube or a two-dimensional channel whose walls are coated with a thin film of the same fluid. This thin film might have been deposited during the displacement of a semi-infinite bubble inside the tube formerly filled with the liquid. In the more general case, the liquid plug propagates on a pre-existing film whose thickness is H_∞^D (the precursor film) and leaves behind the deposited or trailing film with a thickness equal to H_∞^T. If the displacement is steady, H_∞^D and H_∞^T will be equal and their values as well as the length of the plug (L_P) will depend on the relative strength of inertia, viscous, and capillary forces. If the plug length is increased without changing the relative strength of the aforementioned forces, the film thickness of the steady states will asymptotically tend toward a limiting value. At that point we reached a particular situation: the motion of a train of long bubbles where the plug is formed by the liquid located between the rear and front parts of two consecutive bubbles that move without interacting with each other.

Propagation of a single semi-infinite bubble through a capillary tube (or through a two-dimensional channel) initially filled with a Newtonian liquid has been extensively investigated theoretically,[1−3] experimentally,[4−6] and numerically.[7−10] These studies show that the height of the liquid film left behind by the creeping motion of a semi-infinite bubble depends solely on the capillary number ($Ca = \mu U/\sigma$) and on both the capillary and Reynolds numbers when inertia forces are not negligible. More recent studies of this problem deal with the effects of soluble and insoluble surfactants.[11−13]

On the other hand, analysis of the motion of a liquid plug has received less attention. Cassidy et al.[14,15] experimentally studied the flow of a plug in both dried and prewetted tubes. Unfortunately, their results cannot be used to validate our model of short plugs because in one work they considered plugs long enough so that their menisci do not interact and behave as the rear and leading menisci of semi-infinite bubbles while in the other work they studied the influence of surfactants on the speed of a plug propagation.

Recently, Fujioka and Grotberg[16] presented a numerical study of the steady motion of a liquid plug inside a two-dimensional channel lined with a uniform, thin liquid film.

The solutions presented by those authors show the influence of several magnitudes: the inertia forces, the length of the plug (L_P), and the ratio between inertia and capillary forces that is measured by a parameter (λ). They solved the governing equations and appropriate boundary conditions using a finite volume numerical scheme. They showed that for a fixed value of L_P the film thickness increases with the plug propagation speed and that if L_P is larger than the channel width ($2B$), the film thickness agrees well with previous results for propagation of a semi-infinite bubble. They also reported that when $L_P < 2B$ and the inertia forces are not negligible, there is a noticeable interaction between the menisci.

One important issue of the numerical work by Fujioka and Grotberg is that they could not find steady solutions for values of the capillary number larger than 0.4 and $L_P \leq B$. The authors conjectured the possibility that no steady solutions exist under these conditions, but they were not able to confirm this hypothesis because their numerical procedure only solves the steady state.

The objective of the present work is to establish whether a steady-state displacement of a liquid plug inside a capillary tube is stable or not. By stable we mean that if a steady-state solution is perturbed, the system will recover the initial state after a short transient. If after the perturbation the distance between the two menisci either continuously increases or decreases until the collapse occurred, the steady-state solution will be unstable.

The work is organized as follows. We present the mathemati-

* To whom correspondence should be addressed. Tel.: +54 342 4559174. Fax: +54 342 4550944. E-mail: madelia@ceride.gov.ar.
† Universidad Nacional de Entre Ríos.
‡ Universidad Nacional del Litoral.

10.1021/ie0612414 CCC: $37.00
Published on Web 02/16/2007

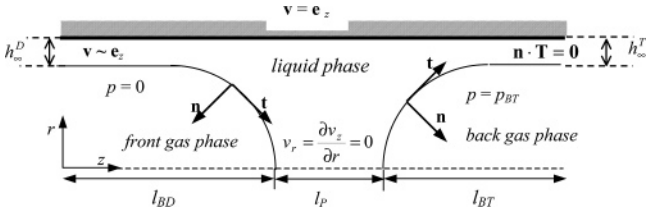

Figure 1. Schematic representation of the flow domain and coordinate system adopted.

cal formulation of the problem in the next section and the main features of the numerical technique employed in section 3. In section 4 we show solutions in order to validate the numerical code and propose a methodology to detect the stability of a steady-state solution. Finally, section 5 is devoted to conclusions.

2. Mathematical Formulation

We consider the propagation of a liquid plug of length L_P in a capillary tube of radius R. The walls of the tube are lined with a film of the liquid whose thickness is equal to H_∞^D. The effect of gravity forces is assumed to be negligible; therefore, the center of the tube is a symmetry line. The gas phases moving ahead and behind the plug may be seen as semi-infinite or very large bubbles; this last situation represents the particular case of a bubble train. Thus, the gas−liquid interfaces delimiting the rear and front regions of the plug correspond to the leading and trailing menisci of these bubbles, respectively. The front meniscus displaces at constant velocity, U, and the coordinate system adopted is moving at the same speed. The gas phase exerts only normal stresses on the interface. The pressure of the gas moving ahead is taken as the reference pressure of the system, and it is arbitrarily set equal to zero, whereas the pressure of the gas phase that is behind the plug is an unknown and must be determined as part of the solution. The gas−liquid surface tension (σ) is constant as well as liquid properties like density (ρ) and viscosity (μ). Figure 1 shows a schematic representation of the flow domain and the coordinate system adopted.

Under the above conditions, the equations governing the liquid flow in the plug are the Navier−Stokes and continuity equations

$$Re\left(\frac{\partial \mathbf{v}}{\partial t} + \mathbf{v}\cdot\nabla\mathbf{v}\right) = -\frac{1}{Ca}\nabla p + \nabla\cdot[\nabla\mathbf{v} + (\nabla\mathbf{v})^{\mathrm{T}}] \qquad (1)$$

$$\nabla\cdot\mathbf{v} = 0 \qquad (2)$$

Equations 1 and 2 are written in dimensionless form using the following scales: U for velocities, R for lengths, R/U for time, and σ/R for pressures; $Ca = \mu U/\sigma$ is the capillary number, and $Re = \rho UR/\mu$ is the Reynolds number.

We assume that the solid wall is impermeable and the liquid adheres there. Far away from the menisci the interface becomes parallel to the solid wall, the films are stagnant, and the thickness of the precursor and trailing films becomes equal to h_∞^D and h_∞^T, respectively. Under steady-state conditions, $h_\infty^D = h_\infty^T$, and this variable is an unknown to be obtained as part of the solution. On the other hand, in a transient solution, the value of h_∞^D is fixed and the thickness of the deposited film is evaluated with the following equation, once the solution of the problem has been computed

$$Q = \int_{A_s} v_z \mathrm{d}A = \pi[1 - (1 - h_\infty^{\mathrm{T}})^2] = \pi h_\infty^{\mathrm{T}}(2 - h_\infty^{\mathrm{T}}) \qquad (3)$$

In eq 3, Q is the liquid flow rate at the outflow plane whose area is A_s.

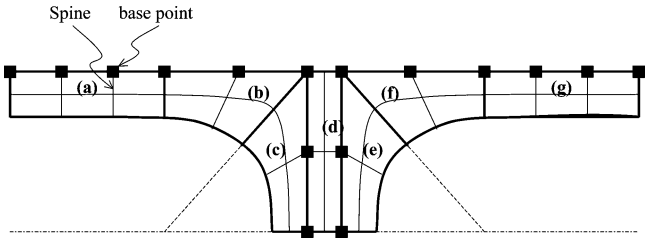

Figure 2. Sketch of the mesh with the distribution of the spines and their base points. The regions of the mesh are also depicted.

The gas−liquid interfaces are material surfaces; therefore, the kinematics condition applies there

$$(\mathbf{v} - \dot{\mathbf{x}}_{\mathrm{SL}})\cdot\mathbf{n} = 0 \qquad (4)$$

$\mathbf{n}$ being the unit normal vector to the free surface (see Figure 1) and $\dot{\mathbf{x}}_{\mathrm{SL}}$ the free surface velocity.

Assuming that the system is free of surface-active agents, the tangential component of the traction at the interface is equal to zero and the normal component is given by the following expression

$$-p\mathbf{n} + Ca\mathbf{n}[\nabla\mathbf{v} + (\nabla\mathbf{v})^{\mathrm{T}}] = (-p_{\mathrm{B}} + 2\mathscr{H})\mathbf{n} \qquad (5)$$

where $\mathscr{H}$ is the local mean curvature of the interface and p_B is the pressure of the gas phase (equal to zero and to p_{BT} ahead and behind of the plug, respectively).

The system of governing equations (eqs 1 and 2) subjected to an appropriate set of boundary conditions is numerically solved using the algorithm that is briefly described in the next section.

3. Numerical Technique

Even though the steady state can be obtained through a transient calculation, we built two numerical codes in order to reduce the computer time: one to solve the steady state and the other to follow the transient response of the liquid plug.

The numerical technique employed in these codes has already been used by the authors to solve steady and transient free surface flow problems.[9,17,18] The technique combines the Galerkin/finite element method with the parametrization of the free surface by means of spines for a convenient spatial discretization of the governing eqs 1 and 2 and their boundary conditions.

The physical domain is tessellated into quadrilateral elements to build the finite element mesh, which is formed by the different regions sketched in Figure 2. Mixed interpolation is used to approximate the velocity and pressure fields, while the coefficients that locate the free surface are interpolated with the one-dimensional specialization of the biquadratic basis functions used for velocities.

The weighted residuals are built in the usual form, and either a set of nonlinear algebraic equations or a set of ordinary differential equations results, depending on whether the steady or transient problem is considered. In the latter case, the set of ordinary differential equations is reduced to a nonlinear one using a finite-difference predictor-corrector scheme.[19]

The resulting system of nonlinear algebraic equations is solved through a Newton loop using the package SuperLU at each iteration.[20] The iterative process is stopped when the norm of the difference between two successive iterations is equal to or smaller than 10^{-6}.

In the transient as well as in the steady case, the dimensionless pressure of the back gas phase is an unknown that is evaluated

with the following equation

$$\mathbf{t} = -\mathbf{e}_r,\ r = 0,\ z = l_{BD} \tag{6}$$

To solve the steady-state problem, the dimensionless film thickness ($h_\infty = h_\infty^D = h_\infty^T$) must be calculated. To this end, the following equation is implemented in the numerical code

$$\mathbf{t} = \mathbf{e}_r,\ r = 0,\ z = l_{BD} + l_P \tag{7}$$

Also, in the steady analysis the velocity profile at the inflow plane is specified as follows. When the free surface becomes parallel to the solid wall, this profile should be flat. However, relaxation of the interface is an asymptotic process, and a small deviation from a plug flow exists in the computational domain even when the inflow plane is located well far away from the meniscus. Thus, at the inflow plane we impose

$$v_z = G(r^2 - 1 - 2r_1^2 \ln r) + 1,\ r_1 \le r \le 1,\ z = 0 \tag{8}$$

where r_1 is the radius of the gas bubble at the entrance. The numerical results show that G is indeed very small and the computed velocity profile is almost flat. In fact, the mean average velocity, $\bar{v}_z$, is equal to 0.99999981 and 0.99999999 for $Ca = 0.5$ and $Re = 50$ and l_P equal to 0.25 and 4.3, respectively. When the last equation is integrated on the inlet area, the following expression relating the constant G with both h_∞ and r_1 is obtained

$$\pi h_\infty(2 - h_\infty) = Q = \int_{A_e} v_z \, dA$$

$$h_\infty(2 - h_\infty) = G\left[2r_1^2 - \frac{1}{2} + r_1^4\left(2 \ln r_1 - \frac{3}{2}\right)\right] + 1 - r_1^2 \tag{9}$$

The velocity and pressure fields, the locations of both interfaces, and the dimensionless pressure of the back gas phase are the unknowns of the transient problem at each time step. In this case, the precursor film thickness, h_∞^D, as well as the velocity profile at the inlet, which is assumed flat, are imposed as essential boundary conditions.

The location of the outflow plane is kept constant during the computations, i.e., the distance l_{BT} is not fixed. The axial length of the elements in the zone indicated as d in Figure 2 increases or diminishes as the distance l_P becomes longer or shorter, respectively, and that of the elements in g varies to fit changes in l_{BT}. The elements located in regions e and f translate as a whole.

To select a finite element mesh we looked for the invariance of the solution with the size of the grid. With this purpose we tested the following two types of meshes: in the coarsest ones the number of elements varies between 1032 and 2400, while in the more refined meshes it varies between 3984 and 6720. In both cases changes are made in the zone labeled d, the total number of elements depending on the value assigned to l_P. Besides, the total number of nodes along the free surfaces is equal to 962 in the finest mesh and 482 in the coarsest one. The solutions computed with these meshes are almost identical; for instance, the relative differences between the computed values of the steady-state film thickness are generally smaller than 0.1% within the whole range of parameters studied in this work, the most noticeable differences being very small variations in pressures and velocities near the inlet region. Nevertheless, the results presented here were computed with meshes of the finer type.

4. Results

The results presented in this section are organized as follows. First, we show some of the numerical tests carried out to validate the numerical codes employed; then, we present solutions for the steady propagation of a liquid plug with the following characteristics: $Ca = 0.5$, $Re \le 50$, and $0.25 \le l_P \le 4.3$, l_P being the distance between the menisci measured in units of R. The value of the capillary number was selected taking into account the maximum value of this parameter at which Fujioka and Grotberg[16] were able to obtain a steady-state solution of the problem for large Re and small l_P. The more relevant parameter of the problem is the film thickness; therefore, the computed values of $h_\infty = h_\infty^D = h_\infty^T$ were depicted as a function of l_P for selected Re. On the basis of the shape of these curves, we speculate about the stability of the steady states computed. Finally, we confirm our conjectures by perturbing a particular steady-state solution and tracing its evolution.

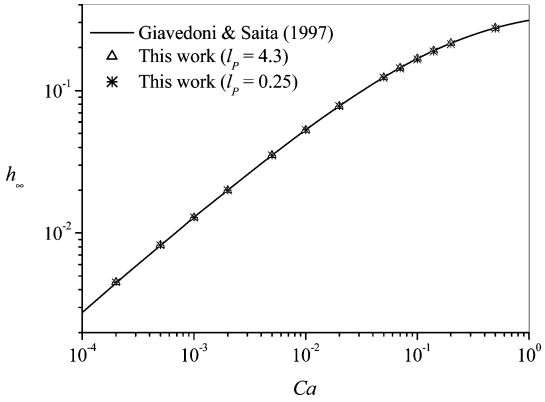

Figure 3. Comparison of the thickness of the deposited and precursor films of a steady plug with that of a semi-infinite bubble for $Re = 0$.

To test the numerical codes described in the previous section, we consider the analysis published by Giavedoni and Saita[9] about the steady displacement of a semi-infinite bubble in a capillary tube initially filled with liquid. As already mentioned, when l_P is sufficiently long, the liquid plug in steady motion is delimited by two gas phases that might be regarded as semi-infinite bubbles; therefore, the thickness of the precursor and deposited films must be independent of the distance between the menisci and should be equal to the thickness of the film deposited by the semi-infinite bubble. Our numerical solutions show that this is the case when $l_P > 4$ for all computations carried out in this work.

From Figure 3 the following conclusions can be drawn: (i) the agreement between the present results and those previously reported is very good, and (ii) the length of the liquid plug has a negligible influence on h_∞ when the inertia forces are meaningless. This last result is similar to that reported by Fujioka and Grotberg[16] in their analysis of the steady displacement of a liquid plug in a 2-D channel, although values reported by these authors for $Ca > 0.05$ show a weak dependence of h_∞ with the length of the plug.

4.1. Steady-State Analysis. In order to analyze the steady state and detect situations in which this type of solution cannot be obtained, we performed numerical calculations for $2 \times 10^{-4} \le Ca \le 0.5$, $0 \le Re \le 250$, and $0.25 \le l_P \le 4.3$; however, just the results for $Ca = 0.5$ will be used here since the focus of this work is to show the procedure employed to determine the plug stability. It is worth noting that we were able to compute the corresponding steady states in the whole range of dimensionless parameters selected; this is an important difference with the work by Fujioka and Grotberg,[16] and it is probably due to the more robust algorithm used here.

As already mentioned, the main goal of this analysis is to develop a methodology in order to detect the stability of a

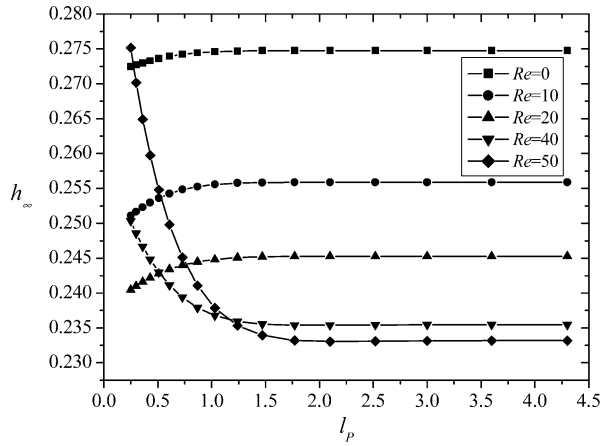

Figure 4. Computed values of the deposited and precursor film thickness of a steady plug as a function of the distance between the menisci for $Ca = 0.5$ and several Re.

steady-state solution. If the steady propagation of a liquid plug is not stable, a perturbation will cause the gas phases to either approach or recede from one another. If this is the case, the thickness of both the deposited and the precursor films must be different because the net flow rate into the plug is different from zero. Although it is clear that a transient analysis is required to trace the evolution of the perturbation, we next show that the stability of the solution can be inferred from the steady-state results.

To this end and based on the above discussion, the trend of h_∞ as a function of Re and l_P for $Ca = 0.5$ was studied. In Figure 4 the film thickness vs the length of the liquid plug is depicted for different values of the Reynolds number. It is easy to note the two different behaviors exhibited by h_∞. In fact, depending on the value of the Reynolds number, this variable increases or decreases with l_P. In the present case, the switch takes place for Re between 20 and 40. It is also worth observing that h_∞ asymptotically approaches a constant value as l_P becomes longer. This value depends only on Re for a fixed Ca and is equal to the film thickness left behind by a semi-infinite bubble.

The two tendencies displayed by h_∞ are the basis of the following conjectures concerning the stability of the system. Consider, for instance, the steady plug with length $= 0.36$ and $Re = 20$. The corresponding film thickness is $h_\infty^D = h_\infty^T = 0.241568$. Now, imagine that somehow a very small amount of liquid is extracted from the plug to perturb the distance between the gas phases. This situation should not affect the precursor film whose thickness (h_∞^D) must be kept constant and equal to 0.241568 but h_∞^T should vary since the plug length has been reduced. Results illustrated in Figure 4 show that the trailing film thickness (h_∞^T) corresponding to a point to the left of the initial condition (i.e., for l_P smaller than 0.36) is somewhat smaller than 0.241568. This difference between h_∞^T and h_∞^D implies that the inflow rate of liquid into the plug is larger than the outflow rate; consequently, the gas phases will move apart and h_∞^T will get thicker until the initial state of the system is recovered.

Consider now the same initial state of the system but instead of pulling out a small amount of liquid from the plug we introduce some liquid into it, forcing a larger separation of the gas phases. The curve for $Re = 20$ (see Figure 4) shows that h_∞^T will become slightly larger than the precursor film thickness; therefore, the volume of the plug will decrease because the inflow rate of liquid is smaller than the outflow rate; thus, the gas phases will approach each other and h_∞^T will get thinner. This process will continue until both films have the same thickness and the initial distance between the menisci ($l_P = 0.36$) is recovered.

From the above discussion we argue that any steady-state solution lying on one of the curves illustrated in Figure 4 with a positive slope ($dh_\infty/dl_P > 0$) represents a stable plug.

When a similar reasoning is applied to a point lying on a concave curve, we conclude that this solution is unstable. Finally, the points at which $dh_\infty/dl_P = 0$ are neutrally stable.

From results depicted in Figure 4, the stability of a train of long bubbles moving steadily in a capillary tube can also be inferred. In this case, the thickness of the film, which is equal to the film thickness left behind by a semi-infinite bubble, can be obtained from the curves drawn in that figure when $l_P > 3.5$. For instance, for $Re = 40$, $h_\infty = 0.235447$. Suppose that some liquid is withdrawn from the plug so that the distance between the bubbles, which is initially larger than 3, becomes equal to 0.36. After the perturbation the thickness of the precursor film remains constant and smaller than h_∞^T (see Figure 4); then, there will be a net flow of liquid out of the plug, h_∞^T will get thicker, the bubbles will come closer, and eventually might collapse.

We can reason in a similar way for a train of bubbles characterized by a smaller Re (e.g., $Re \leq 20$). After perturbation, h_∞^T is smaller than h_∞^D; then, the outflow rate will be smaller than the inflow rate and, consequently, the volume of the plug will increase. If one takes into account the asymptotic behavior of the solution, this process will not end, and strictly speaking, these trains will not be stable. However, in a real situation the relative motion of the bubbles will be negligible when $dh_\infty/dl_P \approx 0$, and these bubble trains could be regarded as stable from a practical point of view.

It is clear that the above speculations must be verified. To this end, we perturbed a steady-state solution and numerically followed its evolution to establish its stability.

4.2. Transient Analysis. The numerical experiments presented here were designed taking into account the previous argument. Starting from a steady-state solution, the distance l_P is 10% either increased or decreased and the back gas phase is allowed to move toward or away from the front gas phase. In the computer code this is fulfilled by imposing h_∞^D as an essential boundary condition while h_∞^T is free to move and is calculated as part of the solution at each time step.

The first experiment corresponds to the hypothetically unstable situation discussed in the above section for a liquid plug characterized by $Re = 40$, $Ca = 0.5$, and $l_P = 0.36$. Figure 5a and b illustrates the evolution of the distance between the menisci and the thickness of both films when the perturbed distance, l_P^t, is set to 1.1 and 0.9 times l_P, respectively.

Results depicted in Figure 5a show that if the volume of the plug is slightly increased, the gas phases move apart and the distance between them increases until the end of the computation. Due to the abrupt change imposed to l_P, the dimensionless film thickness at the outflow plane presents small variations near $t = 0$. This variable then diminishes as the volume of the plug increases until it becomes constant and approximately equal to 0.23430. This occurs at $t \approx 80$ and for $l_P \approx 2.0$. From the curve for $Re = 40$ drawn in Figure 4, it is easy to check that h_∞ is almost independent of l_P when this variable is greater than 2. Once the thickness of the deposited film becomes constant, the motion of both bubbles turns steady and h_∞^T depends only on the particular values of the capillary and Reynolds numbers calculated with the displacement velocity of the back gas phase. From the numerical results illustrated in Figure 5a, the relative velocity between the bubbles when they are moving steadily is

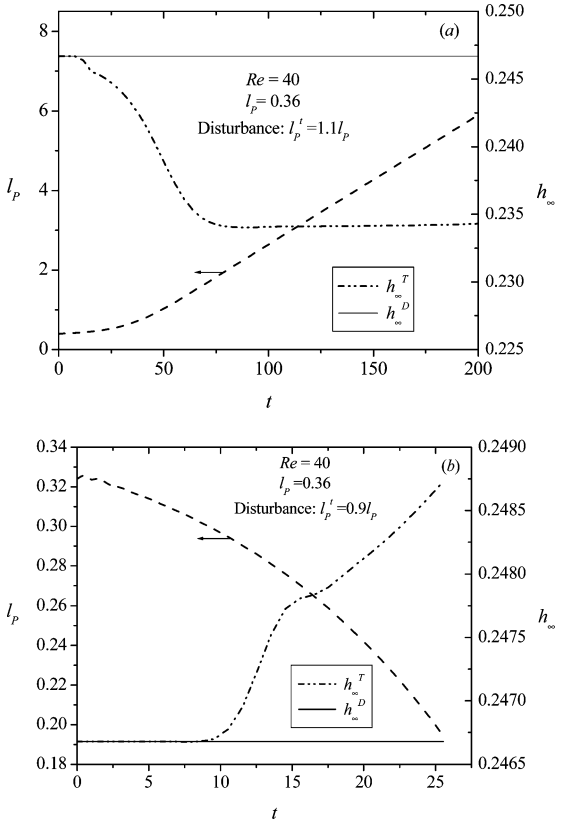

Figure 5. Time evolution of l_P and h_∞^T after a 10% perturbation of the steady-state distance between the menisci. Other parameters of the system are $Re = 40$ and $Ca = 0.5$. The volume of the plug continuously increases (a) or decreases until the collapse (b).

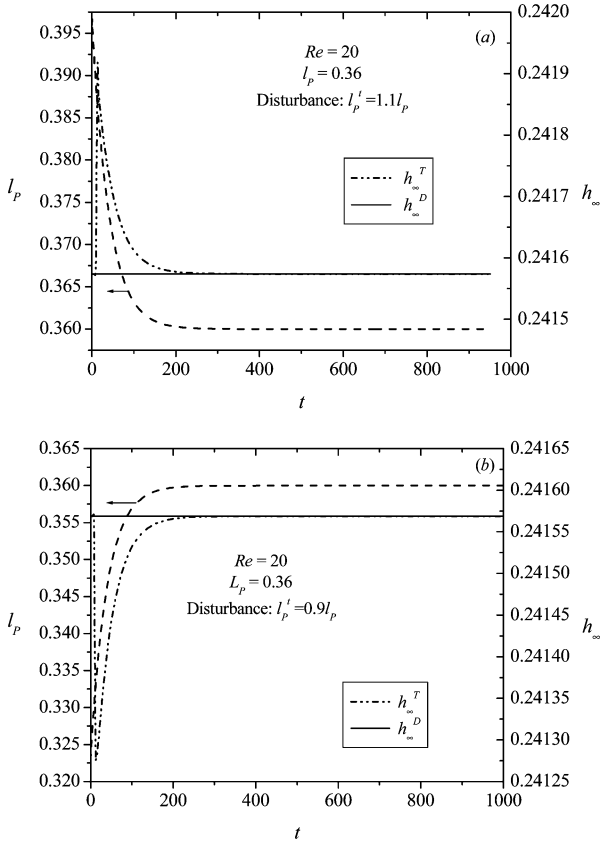

Figure 6. Time evolution of l_P and h_∞^T after a perturbation of the steady-state distance between the menisci. Other parameters of the system are $Re = 20$ and $Ca = 0.5$. The steady-state distance between the bubbles is 10% increased (a) and 10% reduced (b).

$dl_P/dt \approx 0.032$; this signifies that the speed of the trailing bubble has been reduced by approximately 3.2%. Consequently, h_∞^T should be equal to the height of the liquid layer left behind by a semi-infinite bubble characterized by $Ca = 0.484$ and $Re = 38.72$. To check this point, we solved the problem of the semi-infinite bubble for that set of dimensionless parameters and found that the difference between $h_\infty = 0.23414$ and $h_\infty^T = 0.23430$ is 0.072%.

When the volume of the plug is suddenly reduced (see Figure 5b), the distance between the menisci decreases after a very brief interval of time near $t = 0$, during which the bubbles move apart. From the evolution of l_P it is easy to notice that the relative velocity of the gas phases is larger as the bubbles approach each other. An interesting feature of the curves illustrated in this figure is that h_∞^T remains nearly constant up to $t \approx 9$ even though l_P is continuously changing. This fact indicates that the disturbance imposed to l_P is not detected immediately at the outflow plane.

In this and similar events the computation stopped when the distance between the bubbles is too small to be worked out with the mesh adopted.

The second experiment represents the hypothetically stable case previously posed for a liquid plug defined by $Re = 20$, $Ca = 0.5$, and $l_P = 0.36$. Also in this situation the transient analysis confirms our conjectures. In fact, if the steady state is perturbed by adding (Figure 6a) or subtracting (Figure 6b) $0.1 l_P$ to the length of the plug, the initial state is recovered.

An analogous analysis can be applied to study the stability of a bubble train. In this case, the computation is started from one of the steady-state solutions previously obtained in which the distance l_P is large enough to neglect any interaction between the bubbles; $l_P = 4.3$ in the examples discussed in this work. It is worth noticing that the initial distance is largely perturbed setting $l_P^t = 0.36$, a significantly smaller value than l_P. We decided to impose such a large change taking into account the asymptotic behavior exhibited by h_∞ as a function of l_P (see Figure 4). Indeed, we performed computations in which l_P^t was set closer to 4.3 with identical results to those shown here regarding the stability of the train; however, in those situations the relative velocity of the bubbles is so small that a large amount of computer time is required to follow the evolution of the system. In these examples, as previously reported for the plug, h_∞^D (the film thickness left behind by the bubble that is traveling ahead) is imposed as an essential boundary condition while h_∞^T is calculated as part of the solution at each time step using eq 3.

Figure 7a and b depicts the time evolution of the distance between the bubbles and the thickness of the leading and trailing meniscus for $Re = 40$ and 20, respectively. The curves illustrated in the first place show that the steady state is unstable, in agreement with our previous speculation. In fact, the bubbles continuously move toward each other after an initial period of time during which l_P oscillates due to the sudden change imposed. The film thickness of the trailing bubble remains practically constant during the simulation due to the time required by the perturbation to reach the outflow plane; consequently, the values of h_∞^D and h_∞^T appear superimposed in Figure 7a. In order to show the changes undergone by that bubble as it moves forward, the distance between the interface and the tube wall, h, at a distance equal to 2 and 3 from the bubble tip is also depicted. We observe that h becomes thicker as l_P diminishes, indicating that after a certain time this trend will reach the outflow plane changing h_∞^T. Moreover, although changes in h are very similar at both locations, it is clear that

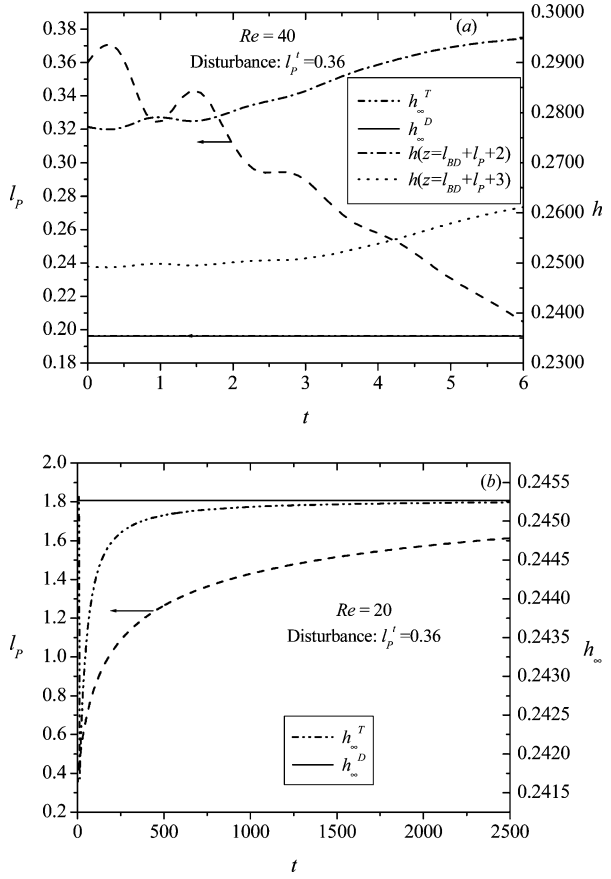

Figure 7. Time evolution of l_P and h_∞^T after a perturbation of a bubble train. The parameters of the system are (a) $Re = 40$ and $Ca = 0.5$ and (b) $Re = 20$ and $Ca = 0.5$.

they are more remarkable nearer the tip, where the influence of the perturbation is first noticed. The computation ends when the distance between the bubbles cannot be resolved with the numerical grid employed ($l_P = 0.20$).

Results illustrated in Figure 7b confirm our previous hypothesis regarding the stability of the bubble train. In fact, when the initial distance between the bubbles ($l_P = 4.3$) is abruptly reduced to $l_P^t = 0.36$, the bubbles move apart with a relative velocity that diminishes as the flow rates of the trailing and leading bubbles become equal. The numerical simulation was deliberately stopped due to the large amount of computer time required to fully recover the initial state.

5. Conclusion

In this paper we presented a numerical solution of the displacement of a liquid plug inside a capillary tube initially lined by a uniform thin liquid film. The numerical technique employed allows computing steady-state solutions within a large range of the dimensionless parameters of the system. In fact, we could solve the problem for $Ca = 0.5$, large Re, and small l_P. A set of conditions at which the technique employed by Fujioka and Grotberg[16] to study the steady propagation of a plug in a two-dimensional channel fails.

Depending on the value of the Reynolds number, two types of curves result when the steady-state values of the film thickness are depicted versus l_P for a fixed Ca. From 0 up to a certain Re, $h_\infty^D = h_\infty^T$ increases with l_P until it becomes practically constant, while for larger Re, this variable first diminishes and then levels off as the distance between the gas phases becomes longer.

We argued how these different trends might be connected with the stability of the plug and confirmed our hypotheses perturbing a given steady-state solution and following its evolution numerically.

Thus, we conclude that it suffices to solve the steady problem to determine whether a steady liquid plug is stable or not. The trend followed by the film thickness as a function of the length of the plug for fixed Re and Ca contains the required information. In fact, a point on a curve for which $dh_\infty/dl_P > 0$ represents a stable steady plug, while a point on a curve for which $dh_\infty/dl_P < 0$ is a liquid plug which is unstable to perturbations. We show that the analysis also applies to the particular case of a bubble train.

Future work on this topic will consider the stability of liquid plugs within a conveniently established range of the dimensionless parameters of the system.

Nomenclature

Dimensionless groups
Ca = capillary number, $\mu U/\sigma$
Re = Reynolds number, $\rho UR/\mu$

Latin symbols
A_S = dimensionless area of the outflow plane
B = one-half of the channel width, m
$\mathscr{K}$ = dimensionless mean surface curvature, m^{-1}
H_∞ = film thickness, m
H_∞^D = precursor film thickness, m
H_∞^T = trailing film thickness, m
h_∞ = dimensionless film thickness
h_∞^D = dimensionless thickness of the precursor film
h_∞^T = dimensionless thickness of the trailing film
l_{BD} = dimensionless length of the front gas phase
l_{BT} = dimensionless length of the back gas phase
L_P = length of the plug, m
l_P = dimensionless plug length
Q = dimensionless flow rate at the outflow plane
$\mathbf{n}$ = outward unit vector normal to the free surface
p = dimensionless pressure
p_B = dimensionless pressure of the gas phase
p_{BT} = dimensionless pressure at the back gas phase
$\mathbf{T}$ = stress tensor, N m^{-2}
t = dimensionless time
$\mathbf{v}$ = dimensionless velocity vector
v_r = r-component of the velocity vector
v_z = z-component of the velocity vector
$\dot{x}_{SL}$ = dimensionless free surface velocity

Greek Symbols
λ = ratio between inertia and capillary forces, Re/Ca
μ = liquid viscosity, kg m^{-1} s^{-1}
ρ = liquid density, kg m^{-3}
σ = surface tension, N m^{-1}

Acknowledgment

The authors greatly acknowledge financial aid from CONICET, ANPCyT, and the Universidad Nacional del Litoral.

Literature Cited

(1) Bretherton, F. P. The motion of long bubbles in tubes. *J. Fluid Mech.* **1961**, *10*, 166.
(2) Park, C. W.; Homsy, G. M. Two phase displacement in Hele-Shaw cells: Theory. *J. Fluid Mech.* **1983**, *139*, 291.

(3) Ratulowski, J.; Chang, H.-C. Marangoni effects of trace of impurities on the motion of long bubbles in capillaries. *J. Fluid Mech.* **1990**, *210*, 303.

(4) Taylor, G. I. Deposition of a viscous fluid on the wall of a tube. *J. Fluid Mech.* **1961**, *10*, 161.

(5) Chen, J. D. Measuring the film thickness surrounding a bubble inside a capillary. *J. Colloid Interface Sci.* **1986**, *109*, 341.

(6) Schwartz, L. W.; Princen, H. M.; Kiss, A. D. On the motion of bubbles in capillary tubes. *J. Fluid Mech.* **1986**, *172*, 259.

(7) Reinelt, D. A.; Saffman, P. G. The penetration of a finger into a viscous fluid in a channel and a tube. *SIAM J. Sci. Stat. Comput.* **1985**, *6*, 542.

(8) Shen, E. I.; Udell, K. S. A finite element study of low Reynolds number two-phase flow in cylindrical tubes. *Trans. ASME J. Appl. Mech.* **1985**, *52*, 253.

(9) Giavedoni, M. D.; Saita, F. A. The axisymmetric and plane cases of a gas phase steadily displacing a Newtonian liquid −A simultaneous solution of the governing equations. *Phys. Fluids* **1997**, *9*, 2420.

(10) Giavedoni, M. D.; Saita, F. A. The rear meniscus of a long bubble steadily displacing a Newtonian liquid in a capillary tube. *Phys. Fluids* **1999**, *11*, 786.

(11) Wassmuth, F.; Laidlaw, W. G.; Coombe, D. A. Calculation of interfacial flows and surfactant redistribution as a gas-liquid interface moves between two parallel plates. *Phys. Fluids A* **1993**, *5*, 1533.

(12) Severino, M.; Giavedoni, M. D.; Saita, F. A. A gas phase displacing a liquid with soluble surfactants out of a small conduit: The plane case. *Phys. Fluids* **2003**, *15*, 2961.

(13) Ghadiali, S. N.; Gaver, D. P., III The influence of non-equilibrium surfactant dynamics on the flow of a semi-infinite bubble in a rigid cylindrical capillary tube. *J. Fluid Mech.* **2003**, *478*, 165.

(14) Cassidy, K. J.; Gavriely, N.; Grotberg, J. B. A rat lung model of instilled liquid transport in the pulmonary airways. *J. Appl. Phys.* **2001**, *90*, 1955.

(15) Cassidy, K. J.; Gavriely, N.; Grotberg, J. B. Liquid plug flow in straight and bifurcating tubes. *J. Biomech. Eng.* **2001**, *123*, 580.

(16) Fujioka, H.; Grotberg, J. B. Steady propagation of a liquid plug in a two-dimensional channel. *J. Biol. Eng.* **2004**, *126*, 567.

(17) Campana, D.; Saita, F. A. Numerical analysis of the Rayleigh instability in capillary tubes−The influence of surfactant solubility. *Phys. Fluids* **2006**, *18*, 022104 1.

(18) Ubal, S.; Giavedoni, M. D.; Saita, F. A. A numerical analysis of the influence of the liquid depth on two dimensional Faraday waves. *Phys. Fluids* **2003**, *15*, 3099.

(19) Gresho, P. M.; Lee, R. L.; Sani, R. L. On the time-dependent solution of the incompressible Navier-Stokes equations in two and three dimensions. In *Recent advances of numerical methods in fluids*; Taylor, C., Morgan, K., Eds.; Pineridge Press: Swansea, U.K., 1979; Vol. 1, Chapter 2, p 27.

(20) Demmel, J. W.; Eisenstat, S. C.; Gilbert, J. R.; Li, X. S.; Liu, J. W. H. A supernodal approach to sparse partial pivoting. *SIAM J. Matrix Anal. Appl.* **1999**, *20*, 720.

Received for review September 22, 2006
Revised manuscript received January 11, 2007
Accepted January 15, 2007

IE0612414